Absolute photoluminescence quantum efficiency measurement of light-emitting thin films

Aaron R. Johnson and Shu-Jen Lee
Macromolecular Science and Engineering Center, University of Michigan, Ann Arbor, Michigan 48109

Julien Klein
Organic and Molecular Electronics Laboratory, Department of Electrical Engineering and Computer Science, University of Michigan, Ann Arbor, Michigan 48109

Jerzy Kanicki[a)]
Organic and Molecular Electronics Laboratory, Department of Electrical Engineering and Computer Science, University of Michigan, Ann Arbor, Michigan 48109 and Macromolecular Science and Engineering Center, University of Michigan, Ann Arbor, Michigan 48109

(Received 8 March 2007; accepted 9 August 2007; published online 7 September 2007)

We developed an integrated monochromatic excitation light source integrating sphere based detection system to accurately characterize the absolute photoluminescence quantum efficiency of commonly used polymer light emitting films without using a reference sample. Our methodology is similar to the method reported by de Mello *et al.* [Adv. Mater. **9**, 230 (1997)] In this Note, we show that the absolute photoluminescence quantum efficiency might only be measured when an appropriate calibration of the spectral variation of the measurement system is done. This calibration is especially important when employing a short excitation wavelength (<400 nm) for common silicon-based detector. © *2007 American Institute of Physics.* [DOI: 10.1063/1.2778614]

Photoluminescence studies monitor the electronic decay of photoexcited molecules. The photoexcited molecule can decay via either radiative or nonradiative processes.[1–3] To quantify the characteristic ratio of the radiative process of a molecule, it is useful to define a number called the photoluminescence quantum efficiency (η_{PL}), which is the ratio of the emitted photons to the absorbed photons.[4,5] The η_{PL} of a compound in a solution is usually determined by comparing it to a standard solution. This method is valid only if the emission and absorption ratios of the standard to the sample can be accurately determined and, for thin films, such a condition is not easily met. The anisotropic films produced by spin casting typically result in angular emission patterns that differ from the standard solution. In addition, accurate determination of the reflectance of a highly scattering thin film may not be possible.[4,5] These issues can be resolved by employing an integrating sphere based detection system, wherein the integrating sphere spatially integrates all radiant flux entering and produced within it. In this Note, we examine a measurement technique used to find the absolute quantum efficiency.

Figure 1(a) shows the photoluminescence quantum efficiency measurement system: an excitation light source with a spectral emission of $\phi_{ex}(\lambda)$ and a detection system with a spectral response of $R_{ds}(\lambda)$. The excitation light source contains a Hg/Xe lamp, a monochromator, and the requisite optics to maximize light throughput while protecting the monochromator gratings from infrared emissions from the lamp. A typical beam entering the integrating sphere has an excitation energy of 0.15–0.3 mW. $\phi_{ex}(\lambda)$ describes the final output of the excitation system at the entrance port of the integrating sphere and is the result of the spectral responses of all the optical components including the lamp, the columnating optics, the monochromator, and the fiber optics.

The detection system consists of an integrating sphere, monochromator, detector, and supporting optics. In the system shown in Fig. 1, either a silicon photodiode or charge coupled device (CCD) can be used. During measurement, the sample is typically mounted in the center of the sphere. For any photon flux $\phi(\lambda)$ entering or generated within the integrating sphere, the spectral response measured by the photodiode or CCD, $S(\lambda)$, to the excitation is the result of a simple geometric response of the detector, $R_{de}(\lambda)$:

$$S(\lambda) = \phi(\lambda) \times R_{de}(\lambda). \tag{1}$$

Calibration of the detection system and determination of the response function $R_{de}(\lambda)$ proceed with a NIST traceable tungsten lamp (OL220C from Optronics Laboratories) with a known spectral irradiance at 50 cm given in W cm^{-2} nm^{-1}, as shown in Fig. 1(b). The known irradiance over the area of the sphere entrance is converted to photon flux. $R_{de}(\lambda)$ is the ratio of the system response to the standard lamp to the known photon flux:

$$R_{de}(\lambda) = S_{std}(\lambda)/\phi_{std}(\lambda), \tag{2}$$

where $S_{std}(\lambda)$ is the measured response in units of counts s^{-1} nm^{-1} and $\phi_{std}(\lambda)$ is the photon flux, given in units of photons s^{-1}. Thus, the units of the detection response are then counts/photon, allowing for the proper conversion of units when this term is used to calibrate the collected spectra. Figure 2 shows the calibration curve of the detection system. The U shape of the calibration curve is mainly contributed from the spectral variation of the blazed grating. According to an approximation to the grating equation, for blazed gratings the strength of a signal is reduced by 50% at two-thirds the blaze wavelength and 1.8 times the blaze wavelength.[6]

[a)]Electronic mail: kanicki@eecs.umich.edu

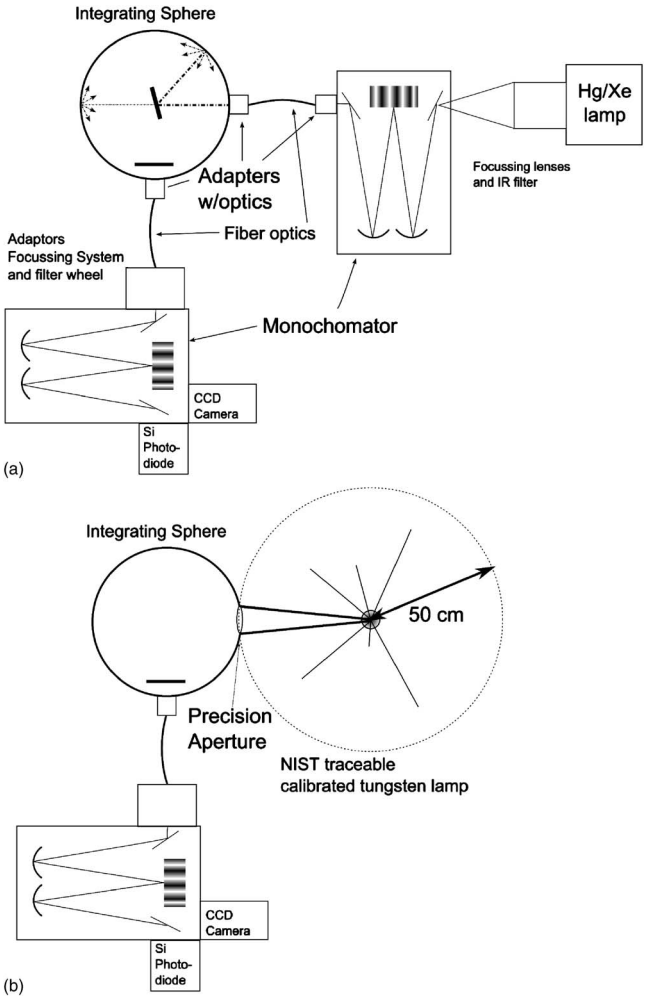

FIG. 1. (a) System schematic for sample measurement. (b) Calibration of detection system with NIST traceable calibrated tungsten lamp at 50 cm from entrance port to integrating sphere.

Since the employed grating (with a groove density of 600 grooves/mm) has a blaze wavelength of 500 nm, its usable range is from 333 to 1000 nm. Therefore, the calibration factors are valid only within this spectral region of this grating. It should also be noted that the spectral responsivity of a standard silicon detector drops below 0.1 A/W at a wavelength shorter than 400 nm.

Once calibrated, the output of the excitation system is connected to the entrance of the integrating sphere and the total photon flux of the excitation light entering the sphere, E_a, is characterized. E_a is determined by shining the excitation light against the sphere wall and integrating the calibrated measured response over the wavelength range of the excitation, λ_{ex}, to find the total number of photons emitting in that region. Hence, the total number of photons entering the sphere, E_a, is found by

$$E_a = \int_{\lambda_{ex}} \phi_{ex}(\lambda) d\lambda. \tag{3}$$

The emission spectrum of the sample and the absorbed excitation flux are characterized in a second measurement in which the sample is placed in the integrating sphere and directly illuminated by the excitation flux. The sample holder was designed in such a way that the light reflecting from a

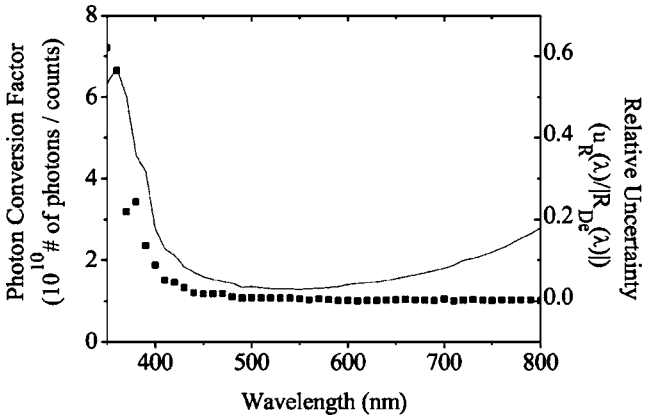

FIG. 2. Calibration function (photon conversion factor) and the relative uncertainty associated with it.

mounted sample will reflect away from the entrance and detection ports. The complete excitation of this measurement is the sum of the unabsorbed excitation light, E_b and the emission light, L_b, less the emission reabsorbed by the sample. The unabsorbed excitation light can be quantified by a similar means as expressed in Eq. (3).

Before quantifying the total emitted flux L_b, self-absorption of the sample must be considered. Since the Stokes shift of emissive polymers is generally small, self-absorption can be a significant source of error for which corrections must be made. The typical method for characterizing self-absorption for lamps, using a broadband auxiliary lamp,[7] is not suitable for PL quantum efficiency measurements as the broad emission will generate photoluminescence in the thin film sample. To correct for self-absorption, a comparison of the spectrum envelopes with and without self-absorption is made by first positioning the sample outside the entrance of the integrating sphere and illuminated with the excitation system. The measured emission does not exhibit the effects of self-absorption. Then, a subsequent scan with the sample inside the sphere is made. The spectra are normalized over a spectral range where self-absorption is expected to be minimal (i.e., longer wavelengths) and the correction factor is found by

$$C_{abs}(\lambda) = \phi'_{out}(\lambda)/\phi'_{in}(\lambda), \tag{4}$$

where $\phi'_{out}(\lambda)$ is the normalized photon flux with the sample out of the integrating sphere, and $\phi'_{in}(\lambda)$ is the normalized photon flux with the sample inside the sphere. The correction factor is taken as a function of wavelength so that it can be applied selectively to the wavelength range of the sample emission and not to the range of the excitation lamp. L_b is then found by

$$L_b = \int_{\lambda_{emit}} \phi_{samp}(\lambda) \times C_{abs}(\lambda) d\lambda, \tag{5}$$

where λ_{emit} is the wavelength range of the sample emission and $\phi_{samp}(\lambda)$ is the photon flux of the remaining excitation flux and the sample emission.

When a sample is excited within the integrating sphere, a fraction A of excitation photons is absorbed by the sample upon first incidence. Therefore, the absorbed photons contribute to an $\eta_{PL}AE_a$ amount of the emission spectrum. As for the unabsorbed photons $[E_a(1-A)]$, the spherical geom-

TABLE I. Uncertainty budget.

Excitation lamp stability	0.5%
Standard lamp	0.32%
Alignment and distance	0.07%
Field Stability	0.31%
Input aperture	0.002%
Spatial uniformity	0.01%
Detector	1.01%
Photometer temperature	0.01%
Sphere reflectance uniformity	1.0%
Monochromator linearity	0.04%
Detector sensitivity uniformity	0.1%
Light leak	0.1%
Sample self-absorption	1.0%

etry and diffuse reflective property of the sphere reflection from the sphere wall result in isotropic illumination of the sample regardless of the sample's position within the sphere. Thus, a fixed fraction μ of the reflected excitation is absorbed by the sample. Secondary absorbed photons then contribute to an $\eta_{\mathrm{PL}}\mu E_a(1-A)$ amount of the emission spectrum in the wavelength range of λ_{emit}. The remaining unabsorbed photons (E_b) will contribute to the resulting spectrum in the same way as the first measurement. The total number of photons absorbed $[E_aA+\mu E_a(1-A)]$ is the difference between the total number of photons entering the sphere and the number of photons not absorbed by the sample: E_a-E_b. With the corrected emission L_b, the PL quantum efficiency can be found by

$$\eta_{\mathrm{PL}} = L_b/(E_a - E_b). \tag{6}$$

The relative uncertainty for this measurement, $U_{\eta_{\mathrm{PL}}}$, follows from the law of propagating uncertainty:[8]

$$U_{\eta_{\mathrm{PL}}} = \left[U_{L_b}^2 + \frac{E_a^2 U_{E_a}^2 + E_b^2 U_{E_b}^2}{(E_a - E_b)^2} \right]^{1/2}, \tag{7}$$

where U_{E_a}, U_{E_b}, and U_{L_b} are the relative uncertainties in excitation flux, unabsorbed photons, and emission flux, respectively.

The uncertainties of this measurement procedure arise from four main sources: the standard lamp and calibration, the detection system, the excitation system used to generate photoluminescence, and the sample itself. An uncertainty budget is shown in Table I.

The alignment of the standard spectral irradiance and its distance from the entrance of the integrating sphere are fixed to a relative uncertainty of 0.07% based on the specifications of optical bench and mount. During calibration, the entrance of the integrating sphere is fitted with a precision aperture with a relative uncertainty of 0.002%. The NIST traceable spectral irradiance standard was calibrated, covering the spectral regions of 200–2500 nm with a typical relative uncertainty in field stability of 0.31% in the visible range and 0.78% in the IR region.[9] At 50 cm along the axis of the lamp, the OL220C, by manufacturer specifications, has a relative uncertainty in spatial uniformity of 0.01%. The combined relative uncertainty for the spectral irradiance standard is 0.32%.

In the detection system, the nonuniform spatial emissions of the thin film sample and the excitation light lead to errors as a result from sphere reflectance nonuniformity. In polymer thin films, where anisotropy cannot be easily predicted or repeated, correction for this nonuniformity is not possible. While the input optics diffuse the excitation light so as to diminish this uncertainty, we estimate the maximum relative uncertainty in uniformity for our measurements at 1%. Spectral mismatch errors are generally not an issue when measuring total spectral radiant flux.[10] Monochromator linearity, light leakage, and detector sensitivity uniformity were determined during manufacturer calibration of the instrumentation to be no greater than 0.04%, 0.01%, and 0.1%, respectively, over the visible range. In our experimental setup, the detector is positioned away from the incident light. As a consequence, the main source of temperature instability comes from heating of the sphere wall, which is quite low. This leads to an estimated relative uncertainty of 0.01%. The combined relative uncertainty for the detection system is no greater than 1.01%.

The relative uncertainties of the excitation system arise from spectral field stability, which is estimated by the manufacturer to be 0.5% across the visible spectrum. The primary source of uncertainty from the sample is self-absorption of emitted photons. We estimate the uncertainty of the self-absorption correction (described above) to be 1%.

To validate the measurement setup, we measured the photoluminescence quantum efficiency of a $10^{-5}M$ solution of rhodamine 6G in ethanol. We compared our data with results from literature. The reported η_{PL} of rhodamine 6G in ethanol is 93%–95% at a solution concentration of $10^{-5}M$ and an excitation wavelength of 492 nm.[11,12] We measured the η_{PL} of rhodamine 6G as 94.33(±3.02%) ($k=2$) which matches very well with accepted values. This measurement technique was also applied to two polymers commonly used in organic electroluminescent devices, orange-emitting poly[2-methoxy-5-(2-ethylhexyloxy)-1,4-phenylenevinylene] (MEH-PPV-POSS) and green-emitting poly(9,9′-dioctylfluorene-alt-benzothiadiazole) (PFBT). The samples were illuminated at 433 and 400 nm for MEH-PPV-POSS and PFBT, respectively. η_{PL} for these polymer thin film were found to be 18.93(±0.56%) ($k=2$) for MEH-PPV-POSS and 47.58(±3.01%) ($k=2$) for PFBT.

[1] N. J. Turro, *Modern Molecular Photochemistry* (Benjamin, New York/Cummings, New York, 1978).
[2] M. Pope and C. E. Swenberg, *Electronic Processes in Organic Crystals* (Clarendon, Oxford, 1982).
[3] M. Yan, L. J. Rothberg, F. Papadimitrakopoulos, M. E. Galvin, and T. M. Miller, Phys. Rev. Lett. **73**, 744 (1994).
[4] J. C. de Mello, H. F. Wittmann, and R. H. Friend, Adv. Mater. (Weinheim, Ger.) **9**, 230 (1997).
[5] N. C. Greenham, I. D. W. Samuel, G. R. Hayes, R. T. Philips, Y. A. R. R. Kessener, S. C. Moratti, A. B. Holmes, and R. H. Friend, Chem. Phys. Lett. **241**, 89 (1995).
[6] J. M. Lerner and A. Thevenon, Jobin Yvon Inc., Edison, NJ, 1988.
[7] CIE Publication No. 25, Central Bureau of the CIE, Vienna, Austria, 1973.
[8] International Organization for Standardization: Guide to the Expression of Uncertainties in Measurements, 1995.
[9] Optronics Laboratories Inc. Bulletin No. 6 (unpublished).
[10] Y. Ohno and Y. Zong, Proceedings of the Symposium on Metrology, 2004 (unpublished).
[11] M. Fischer and J. Georges, Chem. Phys. Lett. **260**, 115 (1996).
[12] J. Arden, G. Deltau, V. Huth, U. Kringel, D. Peros, and K. H. Drexhage, J. Lumin. **48–49**, 352 (1991).